Artificial Melanogenesis by Confining Melanin/Polydopamine Production inside Polymersomes

Claire E. Meyer, Cora-Ann Schoenenberger, Riccardo P. Wehr, Dalin Wu, and Cornelia G. Palivan*

Melanin and polydopamine are potent biopolymers for the development of biomedical nanosystems. However, applications of melanin or polydopamine-based nanoparticles are limited by drawbacks related to a compromised colloidal stability over long time periods and associated cytotoxicity. To overcome these hurdles, a novel strategy is proposed that mimics the confinement of natural melanin in melanosomes. Melanosome mimics are developed by co-encapsulating the melanin/polydopamine precursors L-DOPA/dopamine with melanogenic enzyme Tyrosinase within polymersomes. The conditions of polymersome formation are optimized to obtain melanin/polydopamine polymerization within the cavity of the polymersomes. Similar to native melanosomes, polymersomes containing melanin/polydopamine show long-term colloidal stability, cell-compatibility, and potential for cell photoprotection. This novel kind of artificial melanogenesis is expected to inspire new applications of the confined melanin/polydopamine biopolymers.

1. Introduction

Melanin and melanin-like polydopamine (PDA), based on their propensity to adsorb to a wide variety of materials and absorb UV-visible radiation, have emerged as integral components of potent systems for biomedical applications, e.g., imaging agents, drug carriers, antioxidants or for bone marrow/DNA protection upon irradiation.[1–4] For building melanin-based nanosystems, melanin is usually synthesized in vitro as extraction of melanin from natural sources is complex and

difficult to reproduce. Synthesis pathways involve the oxidation of substrate L-DOPA catalyzed by Tyrosinase to form a heterogeneous melanin biopolymer, while PDA nanoparticles form upon spontaneous oxidation of dopamine.[1,5] Various melanin and PDA-based nanoparticle architectures have been developed depending on their association with other nanomaterials. For example, stabilized emulsion droplets made of primary PDA nanoparticles and polymeric surfactant have led to mesoporous PDA nanoparticles with intrinsic cavities.[6] Different nano objects, e.g., liposomes or polymeric nanospheres have been used as PDA-coated templates to form shell-like or multicompartment structures.[7–10] However, severe drawbacks including compromised colloidal stability, especially over extended periods of time[11] (>3 months) and cytotoxicity when the melanin/PDA biopolymers are exposed at the surface of the particles[12–14] are common to melanin/PDA-based nanosystems.[1,15–17]

In order to solve these drawbacks, we drew inspiration from the architecture and functionality of melanosomes, specialized vesicles in melanocytes that produce and confine native melanin within a phospholipidic membrane and when transferred to the outer skin layer, serve to protect the epidermis from UV-related damages.[18] Here, we present the potential of polymeric vesicles to simultaneously avert aggregation of melanin/PDA and associated cytotoxicity while maintaining UV-absorption properties (**Scheme 1**). Specifically, we investigated the role of confining melanin/PDA in a vesicular compartment, which acts as a shield similarly to melanosomes. In this regard, soft-nanocompartments, i.e., liposomes and polymersomes that, analogous to biological vesicles, consist of a bilayer membrane enclosing an aqueous cavity lend themselves to building melanosome mimics. Polymersomes possess the advantage of increased mechanical stability and broad chemical versatility over liposomes.[19] Moreover, when appropriately selected in terms of the chemical nature of the amphiphilic copolymers, polymersomes are frequently non-toxic and can be combined with a variety of hydrophilic and hydrophobic molecules, be it embedded in their membrane, covalently attached to their external surface or enclosed within their cavity.[19–21] Thus, polymersomes are well suited for many applications including sensing, drug production/delivery, imaging, theranostics and to function as artificial organelles.[19,22]

C. E. Meyer, C.-A. Schoenenberger, R. P. Wehr, C. G. Palivan
Department of Chemistry
University of Basel
Mattenstrasse 24a, Basel 4002, Switzerland
E-mail: cornelia.palivan@unibas.ch
C.-A. Schoenenberger, D. Wu, C. G. Palivan
NCCR-Molecular Systems Engineering
BPR1095, Basel 4058, Switzerland
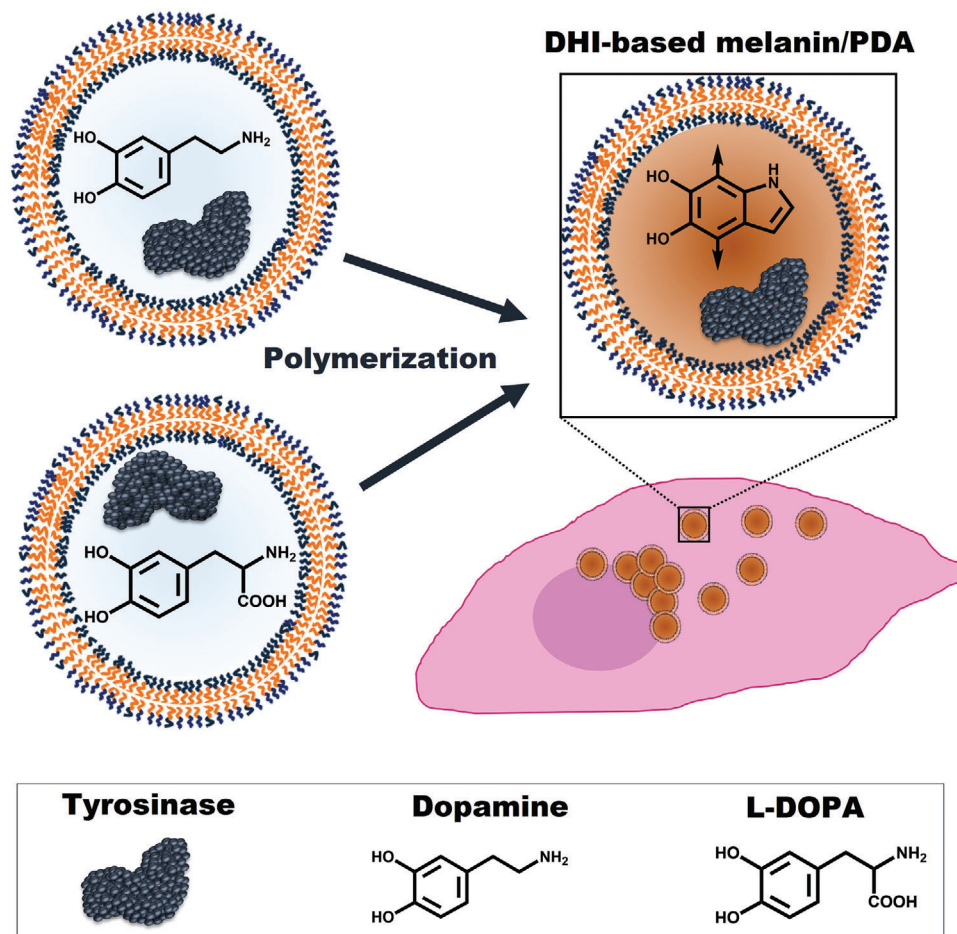
Scheme 1. Polymerization of L-DOPA or dopamine within polymersomes mimicking the maturation of native melanosomes. The polymeric membrane hinders melanin/PDA aggregation that is detrimental to cells. The obtained melanosome mimics, containing 5,6-dihydroxyindole (DHI)-based melanin/PDA, show colloidal stability over an extended period of time, cell-compatibility and the potential for cell-photoprotection.

We developed different melanosome mimics consisting of polymersomes encapsulating melanin or PDA. L-DOPA or dopamine precursors were encapsulated together with Tyrosinase, a key enzyme in melanogenesis, inside polymersomes. Subsequent incubation induced polymerization into melanin or PDA in the compartment inner cavity. To build our polymersomes, we chose a PDMS-b-PMOXA diblock copolymer for its biological compatibility (stealth, non-toxicity), its mechanical stability and impermeability to small molecules.[20,21,23–25] Optimization of several factors including precursor and Tyrosinase concentrations, as well as conditions (temperature and time) of polymersome formation was critical in obtaining such melanosomes mimics. We investigated the differences between Melanin- and PDA-polymersomes in terms of UV-absorption properties, colloidal stability and cytotoxicity. To our knowledge, our system is the first example of melanin and PDA formation within polymersomes where the membrane constitutes a shield against aggregation and cytotoxicity of melanin and PDA while UV-absorption properties are maintained.

Our system sets the stage for a biomimetic strategy based on the encapsulation of melanin/PDA and could represent a prototype of novel melanin/PDA-based nanosystems.

2. Morphological Characterization of Melanosome Mimics

Given the strong tendency of melanin and PDA to unspecifically accumulate on various materials, the formation of polymersome-based melanosome mimics required a strategy where the self-assembly into polymersomes is not impeded by aggregated melanin/PDA polymers. For this reason, we investigated the possibility of encapsulating melanin/PDA precursors (L-DOPA/dopamine) together with Tyrosinase inside polymersomes before their polymerization occurs. While the supramolecular buildup of melanin from precursors remains unclear, its molecular structure has been identified as a heterogeneous macromolecule composed of 5,6-dihydroxyindole (DHI) and 5,6-dihydroxyindole-2-carboxylique acid (DHICA) at various ratios.[26] Tyrosinase is the key enzyme of melanogenesis, as it is involved in several oxidation steps: from the initial precursor L-Tyrosine to L-Dopa, from L-DOPA to DOPAquinone, and later from DHI to indole-5,6-quinone (**Scheme 2**).[27] The steps in between that lead to DHI do not directly involve Tyrosinase as quinones are a highly reactive species that spontaneously undergo a series of chemical reactions involving

ADVANCED
SCIENCE NEWS
www.advancedsciencenews.com

[M] acro-
molecular
Bioscience
www.mbs-journal.de
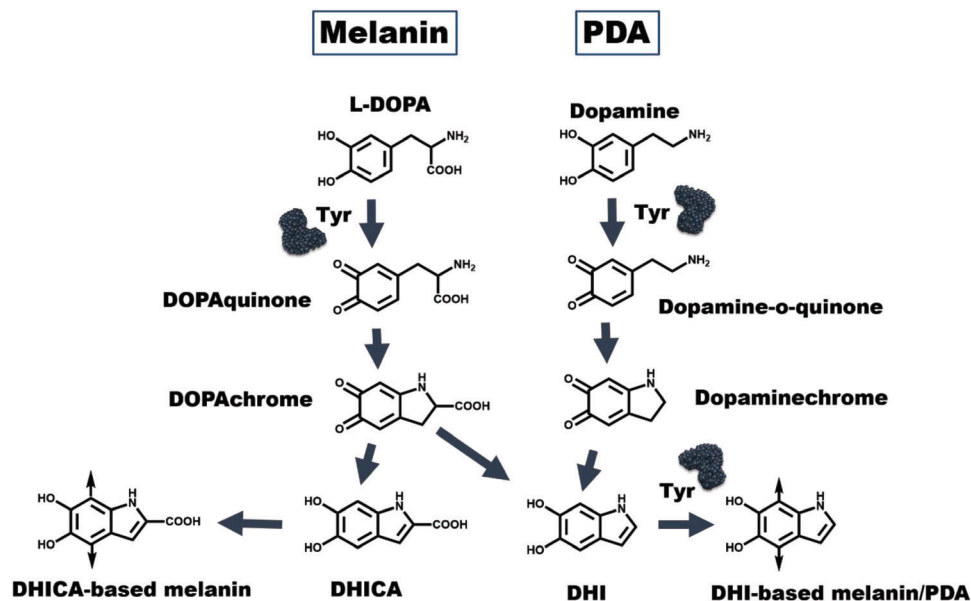
Scheme 2. Pathways of DHICA-based melanin or DHI-based melanin/PDA formation in presence of Tyrosinase.

cyclization and decarboxylation. We chose to encapsulate L-DOPA and dopamine together with Tyrosinase inside polymersomes to form our Melanin-polymersomes and PDA-polymersomes, respectively.

As core component of our artificial melanosome mimic, we synthesized via sequential ionic polymerization the short-chained PDMS$_{24}$-b-PMOXA$_{12}$ to allow for fast self-assembly of polymersomes (Figures S1 and S2, Supporting Information). To initiate self-assembly into melanin- or PDA-polymersomes, a solution of L-DOPA or dopamine was added to a PDMS$_{24}$-b-PMOXA$_{12}$ thin film together with Tyrosinase. Phosphate buffer saline (PBS, pH 7.4) was chosen as rehydration medium primarily because our polymersomes are aimed at biological applications. Further reasons for using PBS are that salts present in the buffer influence the morphology of the resulting self-assembled structures. PBS has been reported to yield polymersomes that are more stable than when self-assembled in water.[28,29] However, under conditions conducive to polymersome formation via the film rehydration method (room temperature for 12 h),[20,30,31] no polymersomes were formed but a brown-black sticky material was obtained which obstructed the stirring (data not shown). Thus, we optimized the time and temperature of film rehydration and concentrations of L-DOPA/dopamine to obtain polymersomes rather than sticky aggregates: rehydration solutions containing concentrations beyond 1×10^{-3} M for L-DOPA/dopamine and 3×10^{-6} M for Tyrosinase were unsuccessful as melanin/PDA polymerization was initiated at the same time as polymersome formation. Hence, conditions were adapted to achieve encapsulation of L-DOPA/dopamine and Tyrosinase into polymersomes prior to polymerization into melanin/PDA: Polymersome formation was carried out at low temperature (4°C) for a short time (30 min). Resulting polymersomes were further extruded and subsequently purified by size exclusion chromatography (SEC) to remove the unencapsulated L-DOPA/dopamine and Tyrosinase. Thus, our optimized preparation method allows for rapid and convenient formation of melanosome mimics without depending on protective atmosphere to prevent L-DOPA/Dopamine oxidation. As previously reported, the ability to rapidly self-assemble into polymersomes also at 4°C arises from the relatively low molecular weight of short-length PDMS-b-PMOXA that reduces steric hindrance amongst the polymer chains.[20] The presence of L-DOPA/dopamine and Tyrosinase affected neither the self-assembly process nor the architecture of the resulting polymersomes, as shown by transmission electron microscopy (TEM) where the typical deflated balloon morphology corresponding to polymersomes was observed. Dynamic light scattering (DLS) showed a diameter of 178 ± 70 nm (polydispersity index, PDI = 0.18) for Melanin-polymersomes and 173 ± 68 nm (PDI = 0.16) for PDA-polymersomes prepared with Tyrosinase, which is consistent with the size of control polymersomes rehydrated with PBS (172 ± 63 nm, PDI = 0.13) or with Tyrosinase only (165 ± 49 nm, PDI = 0.12) under the same conditions (**Figure 1**). Melanin- and PDA-polymersomes prepared without Tyrosinase showed a similar size and morphology (Figure S3, Supporting Information). Additionally, static light scattering (SLS) further confirmed the vesicular nature of all melanosome mimics and control polymersomes (Figure 1 and Figure S3: Supporting Information). The radius of gyration (R_g) of polymersomes was determined, and when dividing it by the hydrodynamic radius (R_h) derived from the DLS profiles, a ratio $0.775 < R_g/R_h \leq 1$ was calculated for all melanin/PDA polymersomes (with and without Tyrosinase) and control polymersomes (empty or encapsulating Tyrosinase alone), which is representative of a hollow spherical morphology.[30] Importantly, our polymersome-based artificial melanosomes fall within the size range of the native organelle, which greatly varies depending on the ethnicity and skin condition (100–800 nm).[18,32,33] Also, the number of Melanin-polymersomes (2.21×10^{12} vesicles mL^{-1}), PDA-polymersomes (2.15×10^{12} vesicles mL^{-1}) (prepared with Tyrosinase) and Tyrosinase-polymersomes (2.14×10^{12} vesicles mL^{-1})

ADVANCED
SCIENCE NEWS
www.advancedsciencenews.com

[M] acro-
molecular
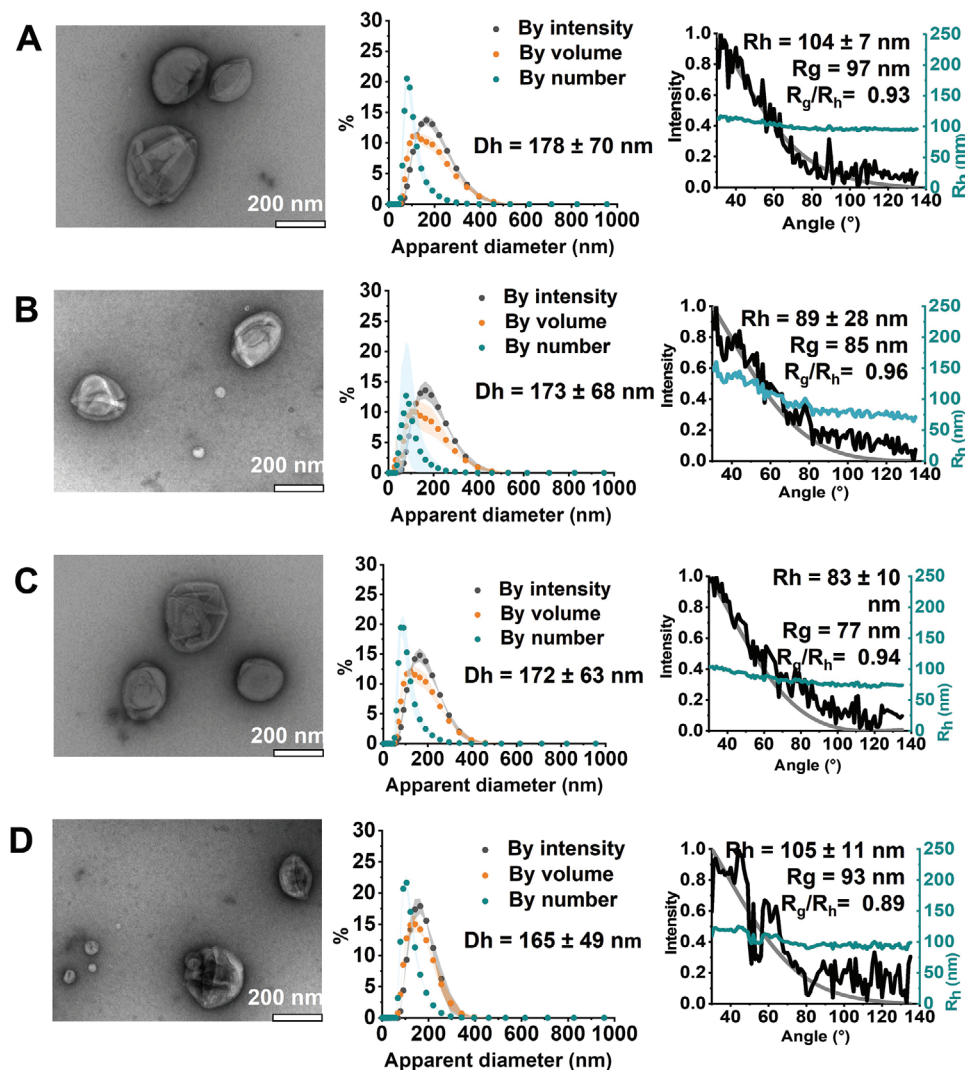Bioscience
www.mbs-journal.de

Figure 1. TEM micrographs and corresponding DLS and SLS revealing the morphology and size of A) Melanin-polymersomes (with Tyrosinase), B) PDA-polymersomes (with Tyrosinase), C) empty polymersomes rehydrated with PBS only, and D) Tyrosinase-polymersomes. SLS data are composed of a DLS profile showing the hydrodynamic radius (R_h) at different angles (cyan), the normalized intensity at different angles (black) and a corresponding MIE fit (grey).

quantified by nanoparticle tracking analysis (NTA) was similar to that of control polymersomes containing only PBS (2.06×10^{12} vesicles mL^{-1}). This indicates that neither L-DOPA/dopamine, nor Tyrosinase interfered with the polymer self-assembly into polymersomes (Table S4, Supporting Information). These results are in agreement with reports indicating that PDMS-*b*-PMOXA polymersomes serve to encapsulate various active compounds and biomolecules.[19,20,34,35]

3. Colloidal Stability of Melanosome Mimics

We chose L-DOPA as melanin precursor as it is rather stable (compared to highly reactive quinone), more soluble than L-Tyrosine, and because the use of downstream precursors like DHI and DHICA is known to decrease the chemical versatility of the oligomers produced as it predisposes the resulting melanin structure toward DHI- or DHICA-derived melanin that

have distinct properties.[11] The structure of PDA differs from that of melanin as in PDA, monomers interact through $\pi-\pi$ stacking and hydrogen bonds rather than covalent bonding.[11,36] Although PDA is formed upon autoxidation of dopamine, we also studied the effect of Tyrosinase on PDA formation within polymersomes.[1,37] We estimated the concentration of encapsulated compounds based on the ratio of the starting concentration (initially used for the self-assembly process of polymersomes formation) and the concentration of unencapsulated compounds determined by measuring the absorbance in the fractions collected from SEC purification (Figure S5, Materials and Methods). We obtained concentrations of L-DOPA (0.13×10^{-3} M), dopamine (0.11×10^{-3} M) and Tyrosinase (0.28×10^{-6} M) for corresponding polymersomes (1 mg mL^{-1}). The resulting encapsulation efficiencies obtained for L-DOPA ($13 \pm 3\%$) and dopamine ($11 \pm 5\%$) were lower than what is usually obtained for encapsulation of small molecules.[38] It is likely that stacking and
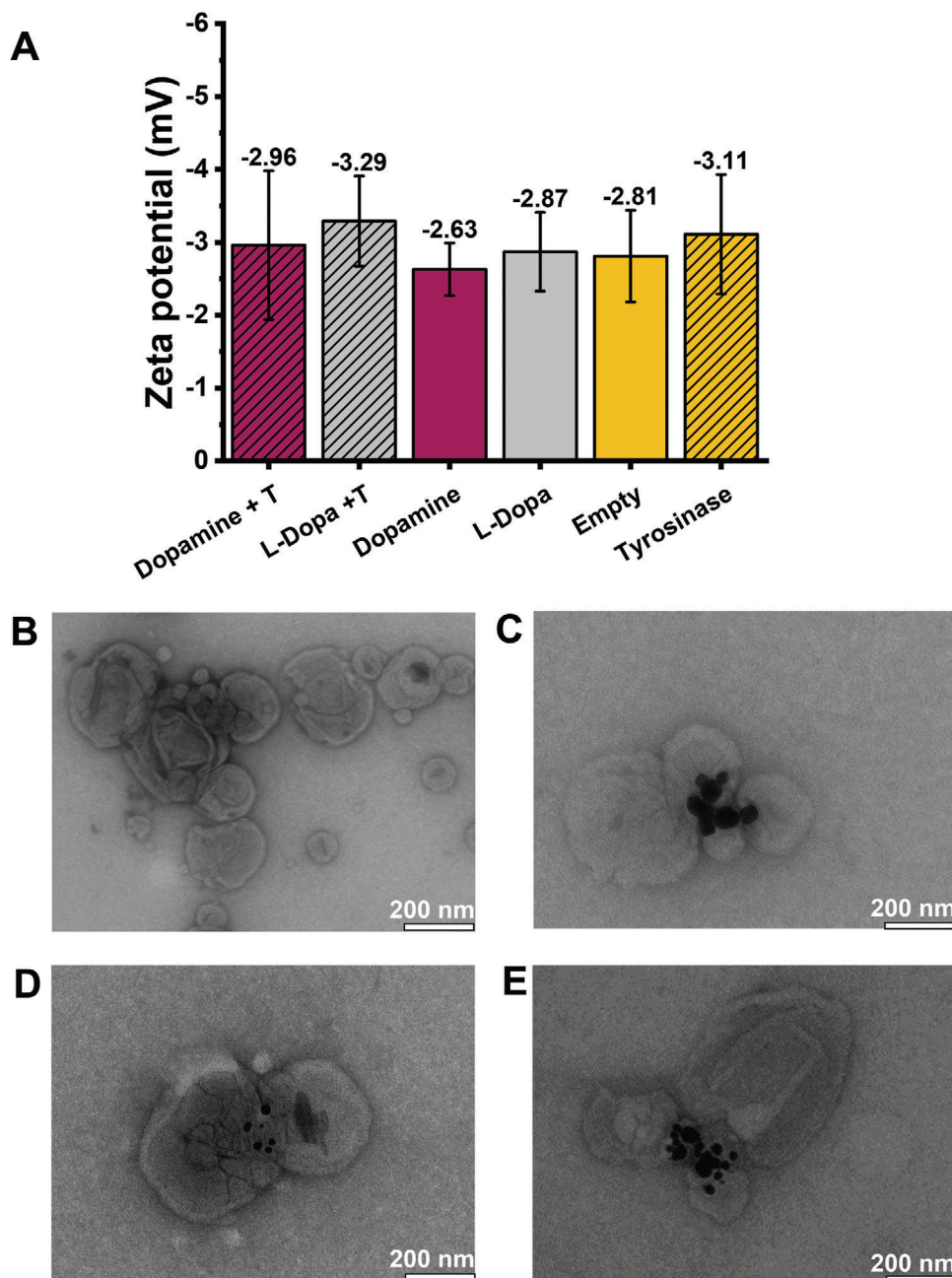
**ADVANCED
SCIENCE NEWS**

www.advancedsciencenews.com

[M] macro-
molecular

Bioscience

www.mbs-journal.de

Figure 2. A) Zeta potential values showing the absence of Dopamine, L-DOPA or Tyrosinase adsorption at the surface of polymersomes. TEM micrographs of polymersome clusters formed after adding B) L-DOPA with Tyrosinase, C) Dopamine with Tyrosinase, D) L-DOPA and E) Dopamine to empty polymersomes.

electrostatic interactions of the respective catecholamines make their encapsulation difficult. In contrast, Tyrosinase encapsulation efficiency ($9 \pm 4\%$) was within the range usually obtained for enzyme encapsulation inside polymersomes.[20,34,39,40] We ruled out the presence of L-DOPA, Dopamine or Tyrosinase adsorbed to the outer surface of polymersomes as similar zeta potentials were obtained for the different melanosome mimics and control polymersomes formed with PBS only (**Figure 2**A). We also performed an experiment where preformed control polymersomes were mixed with low concentrations (100 times lower than the

1×10^{-3} M L-DOPA/dopamine and 3×10^{-6} M Tyrosinase used for film rehydration) of L-DOPA/dopamine (10×10^{-6} M) and Tyrosinase (30×10^{-9} M). The presence of small amounts of L-DOPA and dopamine outside polymersomes resulted in the clustering of polymersomes after one week of incubation at 37°C and extensive aggregates (Figure 2B–E and Figure S6: Supporting Information). In contrast, no aggregation or clustering was observed for the melanosome mimics (kept in similar conditions), corroborating the absence of adsorbed compounds at the surface of polymersomes. Indeed, Melanin-polymersomes and

2100249 (5 of 11)

**ADVANCED
SCIENCE NEWS**

www.advancedsciencenews.com

Macro-
molecular
Bioscience

www.mbs-journal.de

PDA-polymersomes showed high colloidal stability as they maintained their size for at least 6 months of storage at 37°C (Figures S7 and S8, Supporting Information). Hence, by means of encapsulating precursors and Tyrosinase in polymersomes, we introduce a unique approach to preventing melanin and PDA aggregation, which opens new avenues for applying these materials. The colloidal stability of polymersomes not only prevents the light-absorbing biopolymers harbored inside from aggregation, but we expect the polymeric membrane to simultaneously confine melanin- and PDA-associated cytotoxicity while their UV-absorption properties are maintained.

4. UV-Absorption Properties of Melanosome Mimics

Melanin and PDA are known for strong absorption properties, thus broad-brand UV-Vis absorption spectra are considered the cornerstone for monitoring their polymerization.[1,3,36] We examined melanin and PDA formation within the polymersome cavity (with and without co-encapsulated Tyrosinase) by measuring absorbance from 250 to 700 nm up to 24 h (**Figure 3**). The absorption spectrum for all polymersomes encapsulating L-DOPA or Dopamine (with and without Tyrosinase) showed an upward shift indicative of melanin/PDA compared to control polymersomes (empty polymersomes or polymersomes encapsulating only Tyrosinase) where no shifts were obtained even after 24 h (Figure 3). The presence of Tyrosinase (Figure 3D,F) led to an increased absorption for L-DOPA- and Dopamine-polymersomes, showing that the enzyme promotes the production of melanin/PDA. In the absence of Tyrosinase (Figure 3C,E and Figure S9: Supporting Information), a plateau occurred around 450 nm, suggesting that a certain amount of DOPAchrome/Dopamine-chrome did not spontaneously convert (via decarboxylation) into DHI and thus polymerization did not proceed.[41] Indeed, the intramolecular cyclization of Dopa-quinone (via DOPAchrome intermediate) to DHI is known to be very slow.[42] Interestingly, in the presence of Tyrosinase, no unconsumed DOPAchrome/Dopamine-chrome was observed, even though Tyrosinase is not directly involved in the Dopa-quinone to DHI conversion (via DOPAchrome intermediate) (Figure 3D,F).[27] However, Tyrosinase triggers the formation of DOPAchrome precursor (Dopaquinone) and the conversion of the DOPAchrome product (DHI) into reactive indole-5,6-quinone.[27] Conceivably, Tyrosinase affects the DOPAchrome/Dopamine-chrome formation or conversion to DHI by influencing the equilibrium of intermediates resulting from previous or later reaction steps. This hypothesis is supported by the 500 nm absorption shift obtained for L-DOPA polymersomes in presence of Tyrosinase, indicating the formation of DHI-derived melanin (Figure 3D and Figure S9: Supporting Information).[43] Accordingly, a darker coloration of Melanin-polymersome/PDA-polymersomes was visible by eye, consistent with the fast oxidative polymerization of DHI (Figure S9, Supporting Information), as opposed to DHICA-derived melanin that is known to be formed slower and lead to a color-less solution, even after 24 h of reaction.[44] These results support that Tyrosinase favors the formation of DHI-derived melanin rather than DHICA-derived melanin, which is an advantage as DHI-melanin possesses increased visible light absorption properties.[11] Notably, the absorption spectra

of PDA-polymersomes showed stronger absorption compared to melanin-polymersomes over a broad range of wavelengths (Figure 3). This could be explained by a facilitated formation of PDA as it mainly involves fast occurring non-covalent interactions (charge transfer, π-stacking, hydrogen bonding) rather than covalent bonds among units as it is the case for melanin formation.[36] These data suggest an enhanced potency of PDA-polymersomes for UV-absorption applications as compared to Melanin-polymersomes, especially when formed in presence of Tyrosinase (Figure 3).

As the concentration of L-DOPA/dopamine encapsulated in our melanin- and PDA-based melanosome mimics was in the lower range of standard concentrations (25×10^{-6}–100×10^{-3} M) reported for the formation of Melanin and PDA nanoparticles,[45,46] we induced self-assembly of high concentrations of polymer (10 mg mL^{-1}) to obtain concentrated polymersome solutions (around 2×10^{12} vesicles mL^{-1}) that demonstrate light-absorption properties (Table S4: Supporting Information and Figure 3). Furthermore, PDMS-b-PMOXA polymersomes are known to be impermeable to small molecules but allow diffusion of molecular oxygen.[19,47] Thus, encapsulated L-DOPA/dopamine is unable to diffuse out of the polymersome while oxygen can freely diffuse across the polymer membrane and mediate autoxidation or enzyme-catalyzed oxidation of encapsulated compounds, leading to L-DOPA/dopamine polymerization inside the polymersome cavity. Control experiments with free L-DOPA/Dopamine were performed under corresponding conditions, i.e., solutions of L-DOPA/Dopamine ($0.13/0.11 \times 10^{-3}$ M) incubated at 37°C with or without Tyrosinase (3×10^{-6} M) (Figure S10, Supporting Information), to test whether melanin/PDA formation takes place under these conditions (concentrations, temperature, time). We observed a rapid change in color accompanied by aggregation after 12 h, indicating the formation of Melanin/PDA under these conditions (Figure S10, Supporting Information). Similar to the Tyrosinase-related color change observed in polymersome samples, free L-DOPA/dopamine also revealed the enhancing effect of Tyrosinase in obtaining light-absorbing materials.

The evident aggregation of melanin/PDA in solution further demonstrated the low colloidal stability of such materials compared to when encapsulated inside polymersomes (Figure S10, Supporting Information). The aggregation process within polymersomes is most likely terminated by the limited amount of L-DOPA/Dopamine available in the compartment. Aforementioned SLS experiments provided insight on the buildup of melanin/PDA inside polymersomes (Figure 1 and Figure S3: Supporting Information). Particularly, ratios obtained for control polymersomes and melanosome mimics were all within $0.775 < R_g/R_h \leq 1$, indicating a hollow spherical morphology of polymersomes. In other words, consistent with the absence of an optically dense core, polymersomes were not turned into hard spheres in the conditions we used for the polymerization of PDA/melanin in their cavity.[30] Thus, the formation of a single, large melanin/PDA nanoparticle in the polymersome interior can be excluded. Additionally, the values of the R_g/R_h ratio of the melanosome mimics were close to 1, which can be attributed to the low encapsulation efficiency of L-DOPA/dopamine resulting in a limited amount of compounds
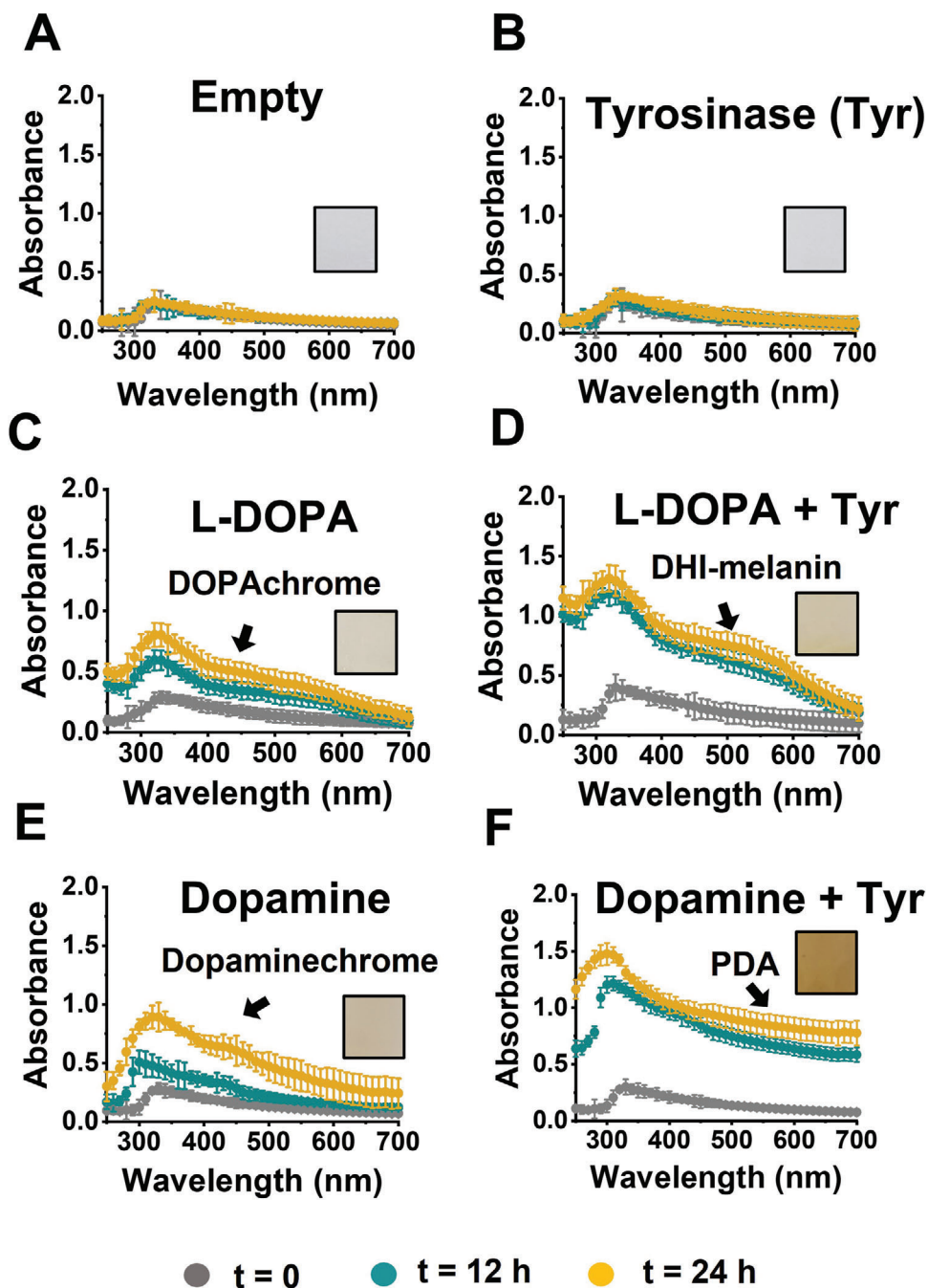
**ADVANCED
SCIENCE NEWS**

www.advancedsciencenews.com

⎰M⎱ **acro-
olecular**

Bioscience

www.mbs-journal.de

Figure 3. Melanin and PDA formation within polymersomes monitored via UV–vis spectroscopy. Absorption spectra measured at $t = 0$ (gray), $t = 12$ h (cyan) and $t = 24$ h (orange) of incubation at 37°C of A) Empty polymersomes, B) Tyrosinase polymersomes, C) L-DOPA polymersomes, D) L-DOPA polymersomes (with Tyrosinase), E) Dopamine polymersomes, F) Dopamine polymersomes (with Tyrosinase). Snapshots illustrate the color of corresponding polymersome solutions after 24 h of incubation (more details in Figure S10, Supporting Information).

available for reaction inside the cavity. We were interested to have low encapsulation efficiency for L-DOPA/dopamine to evaluate the sensitivity of the reaction for low amounts of reactants. Because our melanosome mimics are also impermeable, they are not directly comparable to permeable systems showing lower R_g/R_h, where the confined polymerization reaction relies on a supply of reagents from outside the cavity.[48] Our control polymersomes rehydrated with PBS had an R_g/R_h (0.94) similar to that of Melanin-polymersomes (0.93 with Tyr and 0.96 without) and PDA-polymersomes (0.96 with Tyr and 0.98 without). Thus, we ruled out the possibility of a thick Melanin/PDA coating on the inner surface of the polymersome. As the SLS data excluded the presence of a dense melanin/PDA core or a melanin/PDA coating on the inner polymeric membrane, we
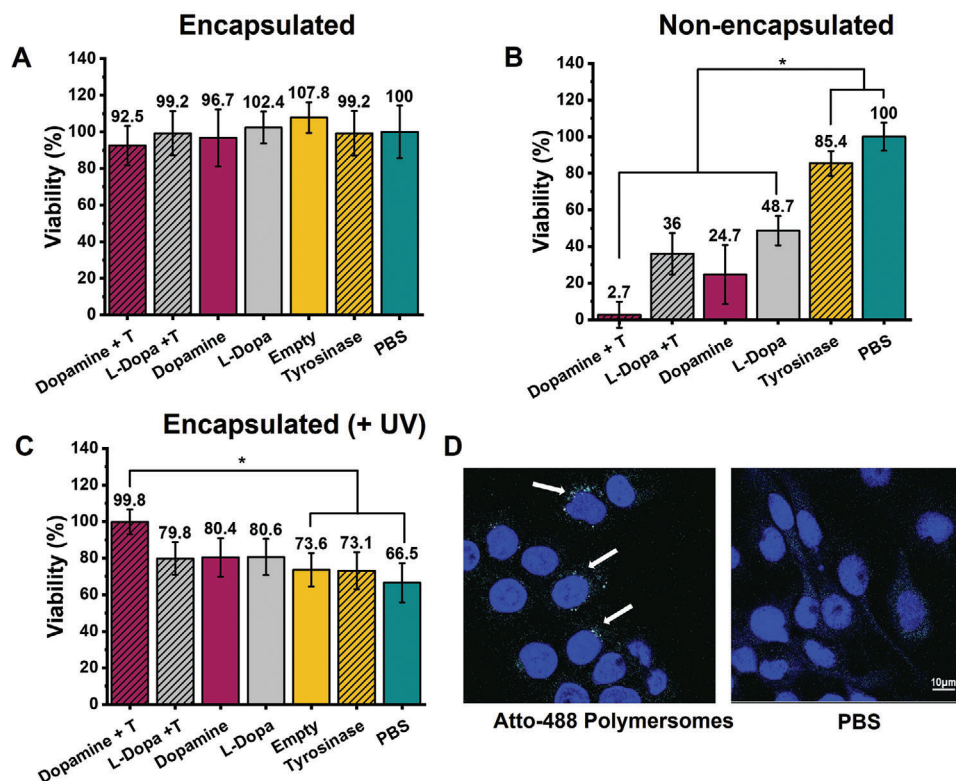
Figure 4. Interaction of polymersome-based melanosome mimics with HaCaT cells. A) Cell proliferation assay showing the non-toxicity of different polymersomes encapsulating dopamine and Tyrosinase (dashed purple), L-DOPA and Tyrosinase (dashed gray), dopamine (purple), L-DOPA (gray), PBS (yellow), Tyrosinase (dashed yellow) compared to control PBS without polymersomes (blue). Cells were incubated with respective polymersomes for 24 h. B) Cell proliferation assay showing the cytotoxicity of free L-DOPA/dopamine (with and without Tyrosinase) compared to PBS. C) Cell proliferation assay showing the cytotoxicity/cell protection effect of different kinds of polymersomes after 40 min of UV-irradiation of cells treated for 24 h with polymersomes. D) CLSM images showing perinuclear localization of model polymersomes (encapsulating fluorescent Atto-488) in keratinocytes. Statistical significance was shown as p values < 0.02.

consider that melanin/PDA within polymersomes was probably present as oligomers and/or lower-nanometer range protoparticles. This notion is in agreement with published data where Tyrosinase-mediated formation of melanin in solution led to 6 nm melanin protoparticles when the reaction was induced in a restricted area.[5,11,49] It should be noted that indirect methods (TEM, DLS, SLS, UV-vis) have been used to characterize our melanosome mimics as their nano dimensions prevent direct imaging. Likewise, the intricate structure of melanin/PDA, as well as its propensity for stickiness and aggregation hamper a structural analysis of the polymersome contents if the bounding membrane were to be extracted. Based on our data showing that by sequestering L-DOPA/dopamine inside polymersomes, production of melanin/PDA with light-absorption properties without large scale aggregation is feasible, and in view of future biomedical applicability of such melanin/PDA-polymersomes, we next addressed the interactions of our melanosome mimics with cells.

5. Cytotoxicity and Potential for Biomedical Applications

Although melanin is a biological pigment and PDA functions in a large variety of bio-applications, both materials show cytotoxicity under certain conditions, e.g., upon UV-irradiation or at increased concentration of the nanoparticles (0.042 mg mL^{-1}).[12–14,50] To assess the cytotoxicity of our melanosome mimics, we carried out cell proliferation assays with the keratinocyte cell line HaCatT (**Figure 4**A) because in the epidermis, mature melanosomes are transferred to keratinocytes where they accumulate around the nucleus to act to protect DNA from UV-radiation damage.[18,33] After incubation of HaCaT cells with polymersomes at high concentration (0.25 mg mL^{-1} of polymer corresponding to 0.5×10^{12} vesicles mL^{-1}, see Table S4: Supporting Information) for 1 day, we did not observe cytotoxicity of our melanin/PDA polymersomes or control polymersomes. In contrast, when we carried out the same experiment with melanin/PDA formed in solution under corresponding conditions, we found significant toxicity compared to PBS or control solution containing only Tyrosinase (Figure 4B and Figure S11: Supporting Information). The apparent cytotoxicity probably arose from the large melanin/PDA aggregates that hinder cell proliferation when no measures are taken to limit the aggregation of melanin/PDA (Figure S12, Supporting Information). Thus, our polymersome-based melanosome mimics, via sequestering of melanin/PDA and prevention of aggregation, eluded cytotoxicity, which renders them suitable for biological applications.

**ADVANCED
SCIENCE NEWS**

www.advancedsciencenews.com

Macro-
molecular

Bioscience

www.mbs-journal.de

Additionally, we tested the cytotoxicity of our melanosome mimics upon 40 min of UV irradiation as melanin and PDA are cytotoxic under certain conditions, e.g., can favor lipid peroxidation when UV-irradiated.[12–14] We observed no increase in cell deaths compared to PBS, suggesting the absence of UV-triggered damaging reactions for our melanosome mimics or control polymersomes (Figure 4C). Notably, in the presence of PDA-polymersomes (with Tyrosinase), we observed an enhanced cell viability compared to control cells. This potential UV-protection activity is indicated by the higher absorption intensity of PDA-polymersomes formed in presence of Tyrosinase (Figure 3) compared to melanin-polymersomes (Figure 4C). Confocal laser scanning microscopy micrographs of HaCaT keratinocytes treated with polymersomes encapsulating Atto-488 fluorescent dye confirmed that our polymersomes have the ability to enter cells where they tend to localize around the nucleus at 24 h of incubation (Figure 4D). This data indicates that our melanosome mimics are a promising alternative for biomedical applications as they demonstrate long-term stability without aggregation, which is a main requirement for translational applications, but are also non-cytotoxic even at high concentration and show the prospective for cell photoprotection.

6. Conclusion

By mimicking the architecture of native melanosomes, polymersomes were exploited to spatially confine melanin/PDA production in order to avoid the main pitfalls associated with melanin/PDA nanoparticles such as aggregation and cytotoxicity.[11] By reproducing for the first time Tyrosinase-mediated melanin synthesis in the confined environment of a soft nanocompartment, i.e., inside polymersomes, we more closely mimic the natural biosynthesis that takes place in melanosomes. For comparison, we produced polydopamine (PDA) within the cavity of polymersomes in a similar fashion, as PDA is the main analogue of melanin and as an emerging biopolymer material with interesting coating properties holds large potential for many applications. By the specific selection of a short-chained PDMS-*b*-PMOXA polymer, our polymersome-based systems showed great colloidal stability, UV-absorption properties as well as the absence of cytotoxicity and a potential for cell photoprotection. The sequestration of melanin/PDA inside polymersomes is a new way of avoiding aggregation, even over extended periods of time that is generally difficult to achieve with melanin/PDA nanoparticles. At the same time, the polymeric membrane enclosing melanin/PDA acts as a barrier preventing cytotoxicity that is associated with non-encapsulated melanin/PDA under certain conditions. Inspired by nature, we provide a new system that side-steps the main drawbacks of melanin/PDA and thus could extend the applicability of these potent macromolecules. Furthermore, the chemical versatility of polymersomes and their numerous possibilities for functionalization greatly extend the range of applications for these biomimetic nanomaterials. For example, with further development, these melanosome mimics could be used as a "healthy" substitute for melanosomes, which are defective in diseases such as Vitiligo or Albinism, and thus could reduce the risk of developing skin cancers.

7. Experimental Section

Materials: All compounds were used as received. Tyrosinase from Mushroom (M_w 138 kDa, pI 4.7 – 5, size 213.53 × 83.72 × 66.95 Å[51]), Dopamine hydrochloride (3,4-dihydroxyphenethylamine -hydrochloride, M_w 189.64 g mol^{-1}) and L-DOPA (3,4-dihydroxy-L-phenylalanine, M_w 197.19 g mol^{-1}) were purchased from Sigma-Aldrich (Buchs, Switzerland). Sterile Dulbecco's PBS (pH 7.4, 0.2 g L^{-1} KCL, 0.2 g L^{-1} KH$_2$PO$_4$, 8 g L^{-1} NaCl, 1.15 g L^{-1} NaH$_2$PO$_4$) suitable for cell assays was purchased from BioConcept (Allschwil, Switzerland).

Synthesis of PDMS$_{24}$-b-PMOXA$_{12}$: Poly(dimethyl siloxane)-*block*-poly(2-methyl-2-oxazoline) (PDMS$_{24}$-*b*-PMOXA$_{12}$) was synthesized following a previously reported protocol.[52] Briefly, hydroxyl-terminated PDMS (PDMS-OH) was obtained after anionic ring-opening polymerization of hexamethylcyclotrisiloxane (13 eq, 0.6 g mL^{-1} in cyclohexane:THF 10:1 V/V) starting from *n*-butyl lithium (1 eq) and end group modification with 2-allyloxyethanol. Subsequently, activation of PDMS-OH (1 eq, 0.1 g mL^{-1} in *n*-hexane) with trifluormethanesulfonic anhydride (1.2 eq) was followed by cationic ring-opening polymerization of MOXA monomer (14 eq). After quenching the polymerization with water and purification by dialysis, the final diblock copolymer was obtained. The average composition and molecular weight (M_w = 2400 g mol^{-1}) were obtained from ^{1}H NMR spectroscopy, and a dispersity of 1.16 was measured by gel permeation chromatography (Supporting Information). Based on previous studies involving cryo-TEM experiments of similar copolymers,[53] and taking into account the specific block ratios, the thickness of the membrane was deduced in PDMS$_{24}$-*b*-PMOXA$_{12}$ vesicles to be 11–11.5 nm.

Preparation of Melanin/PDA Polymersomes: PDMS$_{24}$-*b*-PMOXA$_{12}$ diblock copolymers were dissolved in ethanol to yield a stock solution (10 mg mL^{-1}). 600 µL of this solution were transferred into a 5 mL round-bottom flask and dried in a rotary evaporator (170 mbar, 40 °C, 75 rpm). The resulting thin polymer film was rehydrated with a solution composed of 300 µL of Dopamine or L-DOPA (2×10^{-3} M in PBS) and 300 µL Tyrosinase (6×10^{-6} M in PBS). The resulting solution was stirred for 30 min at 4°C and then extruded (under sterile conditions) 15 times through a polycarbonate (PC) membrane with a 200 nm diameter pore size using an Avanti mini-extruder (Avanti Polar Lipids, Alabama, USA) to unify the size of the polymersomes. Unencapsulated compounds were removed by size-exclusion chromatography (SEC) with cold PBS as mobile phase. Extrusion and SEC purification were carried in a laminar flow hood, using sterile PBS and sterilized extruders, tubings and flasks. The polymersome samples were then placed in an incubator previously disinfected with 70% ethanol, to follow their stability at biologically relevant 37°C.

Preparation of Control Polymersomes: Control polymersomes were prepared as described for melanin/PDA polymersomes (600 µL of 10 mg mL^{-1} PDMS$_{24}$-*b*-PMOXA$_{12}$ solution; 30 min stirring at 4°C) with the following modifications: empty polymersomes were rehydrated with only PBS; Atto-488 polymersomes were rehydrated with 0.2×10^{-3} M of Atto-488 in PBS, Dopamine or L-DOPA polymersomes were rehydrated with PBS (300 µL) and 300 µL of Dopamine or L-DOPA (2×10^{-3} M), respectively.

Dynamic Light Scattering (DLS): The apparent diameters D_H of polymersomes were determined on a Zetasizer Nano ZSP (Malvern Instruments Inc., UK) at 25°C at an angle of 173°. Each sample was diluted with PBS to 0.1 mg mL^{-1} final concentration. A cuvette was filled with 500 µL sample and subjected to 11 runs with three repetitions. As measurements were carried in PBS (pH 7.4, 15 mS cm^{-1}), which is a high conductivity medium, the monomodal mode was employed in the Malvern software (rather than general purpose) to obtain reliable zeta potential data. Under these conditions, no black coloration of the electrodes was observed.

Static Light Scattering (SLS): Multi-angle dynamic light scattering (DLS) and static light scattering (SLS) were performed on a setup from LS Instruments (Switzerland), equipped with a 21 mW He-Ne laser (λ = 632.8 nm) for scattering angles from 30° to 150° at 25°C. All samples were diluted in order to avoid multiple scattering. Second-order cumulant analysis for various angles was performed to obtain the hydrodynamic radius

**ADVANCED
SCIENCE NEWS**

www.advancedsciencenews.com

**Macro-
molecular
Bioscience**

www.mbs-journal.de

(R_h). The radius of gyration (R_g) was obtained from the SLS data using a MIE fit.[30]

Zeta Potential Measurements: The electrophoretic mobility of vesicles in solution was determined by means of laser Doppler velocimetry and phase-analysis light-scattering measurements. A Malvern Zetasizer Nano ZSP (Malvern Instruments Inc, UK) with a 633 nm wavelength laser was used for all measurements. The vesicle samples (0.1 mg mL^{-1}) were measured in PBS with five repeat measurements per sample. All experiments were run at 25°C.

Transmission Electron Microscopy (TEM): 5 µL aliquots of polymersomes (0.1 mg mL^{-1}) were adsorbed to 400 mesh copper grids. Excess liquid was blotted and grids were negatively stained with 2% uranyl acetate. Micrographs of nanostructures were recorded on a Philips CM100 transmission electron microscope at an accelerating voltage of 80 kV.

Estimation of Tyrosinase Encapsulation Efficiency: Tyrosinase polymersomes (Tyrosinase Ncomp) were produced via film rehydration using 300 µL of PBS and 300 µL of Tyrosinase (6×10^{-6} M) under the same conditions as Melanin/PDA polymersomes. The concentration of non-encapsulated Tyrosinase was determined from the fraction of free Tyrosinase present in the solution after size exclusion chromatography (SEC) purification of Tyrosinase Ncomp. After UV-vis absorbance (280 nm) measurements using a NanoDrop 2000 spectrophotometer (Thermofisher), the amount of Tyrosinase molecules encapsulated for 1 mL of polymersomes (1.69×10^{13}) was determined by calculating the difference between the amount of Tyrosinase used for film rehydration and the amount of enzyme that was not encapsulated. In parallel, the concentration of vesicles (2.1×10^{12} vesicles mL^{-1}) was determined via single nanoparticle tracking analysis (NTA) using a NanoSight NS300 instrument from Malvern Analytical (Malvern, United Kingdom). The number of encapsulated Tyrosinase molecules was divided by the number of vesicles, obtaining a value of 8 ± 3 Tyrosinase molecules encapsulated per vesicle. An estimation of the percentage of Tyrosinase encapsulated yielded $9 \pm 4\%$. After SEC purification, a Melanin/PDA polymersome solution of 1 mg mL^{-1} was obtained, corresponding to a Tyrosinase concentration of 0.28×10^{-6} M.

Estimation of Dopamine and L-DOPA Encapsulation Efficiency: Control polymersomes enclosing only Dopamine or L-Dopa (see above) were used to assess the number of Dopamine and L-DOPA molecules per polymersome. The concentration of Dopamine and of L-DOPA encapsulated in 1 mL of polymersomes (1 mg mL^{-1}) was assessed via UV-vis absorbance (280 nm; SpectraMax ID3 microplate reader, Molecular Devices, U.S.A.), by determining the fraction of unencapsulated Dopamine/L-DOPA obtained from SEC purification of polymersomes. In parallel, the concentration of vesicles (1.9×10^{12} vesicles mL^{-1} for Dopamine polymersomes and 1.9×10^{12} vesicles mL^{-1} for L-DOPA polymersomes) was determined via NTA. The total number of encapsulated molecules was divided by the number of vesicles, obtaining a value of $3.8 \times 10^4 \pm 0.4 \times 10^4$ Dopamine molecules/vesicle and $4.4 \times 10^4 \pm 0.3 \times 10^4$ L-DOPA molecules/vesicle. Considering the initial concentration of Dopamine and L-DOPA used for film rehydration (1×10^{-3} M), the percentage of encapsulation was estimated to be $13 \pm 3\%$ for Dopamine and $11 \pm 5\%$ for L-DOPA. Based on this encapsulation efficiency, the concentration of Dopamine and L-DOPA in concentrated solutions (1 mg mL^{-1}) of Dopamine and L-DOPA polymersomes was estimated to be 0.11×10^{-3} M and of 0.13×10^{-3} M, respectively.

Control Experiment for Surface Adsorption of L-DOPA/Dopamine: Preformed empty polymersomes (1 mg mL^{-1}) were mixed with L-DOPA/Dopamine (final concentration of 10×10^{-6} M), with and without Tyrosinase (final concentration of 30×10^{-9} M), and incubated at 37°C for up to 1 week. The concentrations chosen were 100 times lower than those used for film rehydration of polymersomes.

Kinetic Assays: The PDA and melanin polymerization within polymersomes at 37°C was monitored by UV-vis absorbance spectra (250 – 700 nm, measurement every 10 nm; SpectraMax ID3 microplate reader, Molecular Devices, U.S.A.) up to 24 h. 200 µL of 1 mg mL^{-1} polymersomes (directly after their formation) were added to each well of a 96-well microplate (UV-Transparent plates, Corning, USA) and triplicates were measured for each condition. The kinetics of formation of free poly-

dopamine/melanin could not be followed with this method as it rapidly led to the sedimentation of aggregates.

Cell Culture: HaCaT cells (immortalized human keratinocytes) were routinely cultured in DMEM medium (Gibco Life Sciences) supplemented with glucose (4.5 g L^{-1}), L-glutamine (2×10^{-3} M) and 10% fetal bovine serum (BioConcept), penicillin (100 units mL^{-1}) and Streptomycin (100 µg mL^{-1}). Cells were maintained at 37°C in a humidified atmosphere with 5% CO$_2$.

Cell Viability Assay: PrestoBlue (Invitrogen) was used to determine cell viability according to the supplier's protocol. HaCaT cells were seeded at a concentration of 7500 cells/well in a 96 well plate (200 µL final volume). After 24 h, 100 µL of medium were removed and replaced by 75 µL of fresh medium and 25 µL of different polymersomes (initial solutions of 2 mg mL^{-1} of polymer for a final concentration of 0.25 mg mL^{-1} of polymer and a final quantity of 0.05 mg of polymer, corresponding to 0.5×10^{12} vesicles mL^{-1}) or PBS in control wells. Each condition was tested in quadruplicate. Subsequently cells were cultured at 37°C for 1 day in the presence of polymersomes, free L-DOPA/Dopamine ($0.13/0.11 \times 10^{-3}$ M), or control PBS. After 24 h, PrestoBlue reagent (20 µL) was added to each well and after 1 h at 37°C, the fluorescence at 615 nm was measured using a Spectramax plate reader. The data was normalized to PBS treated control cells.

Cell Viability Assay upon UV-Irradiation: As described for the cell viability assay without UV-irradiation, cells were incubated in presence of polymersomes for 1 day. After rinsing 3 times with PBS (200 µL) to remove non-uptaken polymersomes, 100 µL of PBS with Ca^{+2}/Mg^{2+} were added for UV-irradiation in the cell culture hood. Unlidded plates were placed at 80 cm distance from 2 × 2 UV-C 15 W lamps (Osram HNS 15 W G13) with a main emission at 254 nm and irradiated for 40 min. Control plates treated with corresponding polymersomes/PBS were incubated at room temperature for 40 min. PBS was removed and fresh culture medium (100 µL) was added. After overnight culture, cell viability was determined using PrestoBlue reagent as described above. The data was normalized to cells treated in parallel but without irradiation.

Cell Imaging: HaCaT cells were seeded and incubated under the same conditions as described for cell viability assays expect that model polymersomes encapsulating Atto-488 dyes were used. After 24 h of incubation in the presence of polymersomes, cells were rinsed 3 times with PBS to remove non-uptaken polymersomes prior to imaging with a Zeiss LSM 880 inverted microscope (Zeiss Axio Observer, Carl Zeiss, Germany) with a water immersion objective C-Apochromate 40x/1.2 W korr FCS M27. The beam from 488 nm argon laser was passed through a main beam splitter MBS488 and the detection window was from 499–643 nm.

Supporting Information

Supporting Information is available from the Wiley Online Library or from the author.

Conflict of Interest

The authors declare no conflict of interest.

Data Availability Statement

The repository is Zenodo and the DOI is 10.5281/zenodo.5463929 (https://zenodo.org/record/5463929#.YTXLD9-xU2w).

Keywords

[1] V. Ball, *Front. Bioeng. Biotechnol.* **2018**, *6*, 109.

[2] B. Silvestri, G. Vitiello, G. Luciani, V. Calcagno, A. Costantini, M. Gallo, S. Parisi, S. Paladino, M. Iacomino, G. D'errico, M. F. Caso, A. Pezzella, M. D'ischia, *ACS Appl. Mater. Interfaces* **2017**, *9*, 37615.

[3] A. D. Schweitzer, E. Revskaya, P. Chu, V. Pazo, M. Friedman, J. D. Nosanchuk, S. Cahill, S. Frases, A. Casadevall, E. Dadachova, *Int. J. Radiat. Oncol., Biol. Phys.* **2010**, *78*, 1494.

[4] M. E. Lynge, R. Van Der Westen, A. Postma, B. Städler, *Nanoscale* **2011**, *3*, 4916.

[5] O. I. Strube, A. Büngeler, W. Bremser, *Biomacromolecules* **2015**, *16*, 1608.

[6] F. Chen, Y. Xing, Z. Wang, X. Zheng, J. Zhang, K. Cai, *Langmuir* **2016**, *32*, 12119.

[7] A. K. Awasthi, S. Gupta, J. Thakur, S. Gupta, S. Pal, A. Bajaj, A. Srivastava, *Nanoscale* **2020**, *12*, 5021.

[8] W. Zong, Y. Hu, Y. Su, N. Luo, X. Zhang, Q. Li, X. Han, *J. Microencapsulation* **2016**, *33*, 257.

[9] S. Mei, Z. Kochovski, R. Roa, S. Gu, X. Xu, H. Yu, J. Dzubiella, M. Ballauff, Y. Lu, *Nano-Micro Lett.* **2019**, *11*, 83.

[10] R. Van Der Westen, L. Hosta-Rigau, D. S. Sutherland, K. N. Goldie, F. Albericio, A. Postma, B. Städler, *Biointerphases* **2012**, *7*, 8.

[11] A. Büngeler, B. Hämisch, O. Strube, *Int. J. Mol. Sci.* **2017**, *18*, 1901.

[12] S. Ito, K. Wakamatsu, *Photochem. Photobiol.* **2008**, *84*, 582.

[13] J. D. Simon, D. N. Peles, *Acc. Chem. Res.* **2010**, *43*, 1452.

[14] C. Nieto, M. A. Vega, J. Enrique, G. Marcelo, E. M. Martín Del Valle, *Cancers* **2019**, *11*, 1679.

[15] A. Chassepot, V. Ball, *J. Colloid Interface Sci.* **2014**, *414*, 97.

[16] K.-Y. Ju, Y. Lee, S. Lee, S. B. Park, J.-K. Lee, *Biomacromolecules* **2011**, *12*, 625.

[17] L. Panzella, G. Gentile, G. D'errico, N. F. Della Vecchia, M. E. Errico, A. Napolitano, C. Carfagna, M. D'ischia, *Angew. Chem., Int. Ed. Engl.* **2013**, *52*, 12684.

[18] C. Wasmeier, A. N. Hume, G. Bolasco, M. C. Seabra, *J. Cell Sci.* **2008**, *121*, 3995.

[19] C. E. Meyer, S.-L. Abram, I. Craciun, C. G. Palivan, *Phys. Chem. Chem. Phys.* **2020**, *22*, 11197.

[20] C. E. Meyer, J. Liu, I. Craciun, D. Wu, H. Wang, M. Xie, M. Fussenegger, C. G. Palivan, *Small 16*, **2020**, 1906492.

[21] C. G. Palivan, R. Goers, A. Najer, X. Zhang, A. Car, W. Meier, *Chem. Soc. Rev.* **2016**, *45*, 377.

[22] L. Zartner, M. S. Muthwill, I. A. Dinu, C.-A. Schoenenberger, C. G. Palivan, *J. Mater. Chem. B* **2020**, *8*, 6252.

[23] X. Zhang, P. Zhang, *Curr. Med. Chem.* **2017**, *13*, 124.

[24] T. Anajafi, S. Mallik, *Ther. Delivery* **2015**, *6*, 521.

[25] A. Najer, D. Wu, D. Vasquez, C. G. Palivan, W. Meier, *Nanomedicine* **2013**, *8*, 425.

[26] P. Meredith, T. Sarna, *Pigm. Cell Res.* **2006**, *19*, 572.

[27] H. Ando, H. Kondoh, M. Ichihashi, V. J. Hearing, *J. Invest. Dermatol.* **2007**, *127*, 751.

[28] D. J. Adams, M. F. Butler, A. C. Weaver, *Langmuir* **2006**, *22*, 4534.

[29] J. E. Bartenstein, J. Robertson, G. Battaglia, W. H. Briscoe, *Colloids Surf., A* **2016**, *506*, 739.

[30] D. Daubian, J. Gaitzsch, W. Meier, *Polym. Chem.* **2020**, *11*, 1237.

[31] J. Liu, V. Postupalenko, S. Lörcher, D. Wu, M. Chami, W. Meier, C. G. Palivan, *Nano Lett.* **2016**, *16*, 7128.

[32] K. Konrad, *Arch. Dermatol.* **1973**, *107*, 853.

[33] H.-Y. Thong, S.-H. Jee, C.-C. Sun, R. E. Boissy, *Br. J. Dermatol.* **2003**, *149*, 498.

[34] C. E. Meyer, I. Craciun, C.-A. Schoenenberger, R. Wehr, C. G. Palivan, *Nanoscale* **2021**, *13*, 66.

[35] A. Belluati, I. Craciun, C. G. Palivan, *ACS Nano* **2020**, *14*, 12101.

[36] F. Solano, *Int. J. Mol. Sci.* **2017**, *18*, 1561.

[37] L. G. Fenoll, J. N. Rodríguez-López, R. Varón, P. A. Garciá-Ruiz, F. Garciá-Cánovas, J. Tudela, J. Tudela, *Int. J. Biochem. Cell Biol.* **2002**, *34*, 1594.

[38] N. Aibani, T. N. Khan, B. Callan, *Int. J. Pharm.* **2019**, *2*.

[39] S. Iqbal, M. Blenner, A. Alexander-Bryant, J. Larsen, *Biomacromolecules* **2020**, *21*, 1327.

[40] A. Belluati, I. Craciun, J. Liu, C. G. Palivan, *Biomacromolecules* **2018**, *19*, 4023.

[41] B. Manandhar, A. Wagle, S. H. Seong, P. Paudel, H.-R. Kim, H. A. Jung, J. S. Choi, *Antioxidants* **2019**, *8*, 240.

[42] M. D'ischia, A. Napolitano, V. Ball, C.-T. Chen, M. J. Buehler, *Acc. Chem. Res.* **2014**, *47*, 3541.

[43] L. Ascione, A. Pezzella, V. Ambrogi, C. Carfagna, M. D'ischia, *Photochem. Photobiol.* **2013**, *89*, 314.

[44] M. Sugumaran, J. Evans, S. Ito, K. Wakamatsu, *Int. J. Mol. Sci.* **2020**, *21*, 19.

[45] A. Karan, E. Khezerlou, F. Rezaei, L. Iasemidis, M. A. Decoster, *Polymers* **2020**, *12*, 2483.

[46] M. A. Vega, C. Nieto, G. Marcelo, E. M. Martín Del Valle, *Colloids Surf., B* **2018**, *167*, 284.

[47] A. Lanzilotto, M. Kyropoulou, E. C. Constable, C. E. Housecroft, W. P. Meier, C. G. Palivan, *J. Biol. Inorg. Chem.* **2018**, *23*, 109.

[48] M. V. Dinu, M. Spulber, K. Renggli, D. Wu, C. A. Monnier, A. Petri-Fink, N. Bruns, *Macromol. Rapid Commun.* **2015**, *36*, 507.

[49] O. I. Strube, A. Büngeler, W. Bremser, *Macromol. Mater. Eng.* **2016**, *301*, 801.

[50] Y. Deng, W.-Z. Yang, D. Shi, M. Wu, X.-L. Xiong, Z.-G. Chen, S.-C. Wei, *NPG Asia Mater* **2019**, *11*, 39.

[51] S. G. Mauracher, C. Molitor, R. Al-Oweini, U. Kortz, A. Rompel, *Acta Crystallogr. Sect. D: Struct. Biol.* **2014**, *70*, 2301.

[52] D. Wu, M. Spulber, F. Itel, M. Chami, T. Pfohl, C. G. Palivan, W. Meier, *Macromolecules* **2014**, *47*, 5060.

[53] F. Itel, M. Chami, A. Najer, S. Lörcher, D. Wu, I. A. Dinu, W. Meier, *Macromolecules* **2014**, *47*, 7588.

2100249 (11 of 11)